52nd AIAA/ASME/ASCE/AHS/ASC Structures, Structural Dynamics and Materials Conference
 19th
4 - 7 April 2011, Denver, Colorado

AIAA 2011-1890

Analysis of Membrane Dynamics using Multi-Particle Model for Solar Sail Demonstrator "IKAROS"

Yoji Shirasawa[1]
Japan Space Exploration Agency (JAXA), Sagamihara, 252-5210, Japan

Osamu Mori[2],
Japan Space Exploration Agency (JAXA), Sagamihara, 252-5210, Japan

Yasuyuki Miyazaki[3],
Nihon University, Funabashi, 274-8501, Japan

Hiraku Sakamoto[4],
Tokyo Institute of Technology, Tokyo, 152-8552, Japan

Mitsue Hasome[5],
Tokai University, Hiratsuka, 252-1292, Japan

Norizumi Okuizumi[6] and Hirotaka Sawada[7],
Japan Space Exploration Agency (JAXA), Sagamihara, 252-5210, Japan

Hiroshi Furuya[8],
Tokyo Institute of Technology, Yokohama, 226-8502, Japan

Saburo Matsunaga[9],
Tokyo Institute of Technology, Tokyo, 152-8552, Japan

Michihiro Natori[10],
Waseda University, Tokyo, 169-8555, Japan

and

Jun'ichiro Kawaguchi[11]
Japan Space Exploration Agency (JAXA), Sagamihara, 252-5210, Japan

[1] Post-doctoral Researcher, JAXA Space Exploration Center, 3-1-1 Yoshinodai, Chuo-ku, Sagamihara, Kanagawa, Japan.
[2] Assistant Professor, JAXA Space Exploration Center, 3-1-1 Yoshinodai, Chuo-ku, Sagamihara, Kanagawa, Japan.
[3] Professor, Department of Aerospace Engineering, 7-24-1 Narashinodai, Funabashi, Chiba, Japan.
[4] Assistant Professor, Department of Mechanical and Aerospace Engineering, 2-12-1 Ookayama, Meguro-ku, Tokyo, Japan.
[5] Graduate Student, Department of Aeronautics and Astronautics, 4-1-1 Kitakaname, Hiratsuka, Kanagawa, Japan.
[6] Assistant Professor, Institute of Space and Astronautical Science, 3-1-1 Yoshinodai, Chuo-ku, Sagamihara, Kanagawa, Japan.
[7] Post-doctoral Fellow, JAXA Space Exploration Center, 3-1-1 Yoshinodai, Chuo-ku, Sagamihara, Kanagawa, Japan.
[8] Associate Professor, Department of Built Environment, 4259-G3-6, Nagatsuta, Midori-ku, Yokohama, Japan.
[9] Associate Professor, Department of Mechanical and Aerospace Engineering, 2-12-1 Ookayama, Meguro-ku, Tokyo, Japan.
[10] Visiting Professor, Faculty of Science and Engineering, 55S-608, 3-4-1 Okubo, Shinjyuku, Tokyo, Japan.
[11] Professor, JAXA Space Exploration Center, 3-1-1 Yoshinodai, Chuo-ku, Sagamihara, Kanagawa, Japan.

Japan Exploration Agency (JAXA) launched a powered solar sail "Interplanetary Kite-craft Accelerated by Radiation Of the Sun (IKAROS)" on May 21, 2010. One of the primal technologies demonstrated at IKAROS is the deployment of the sail whose diameter is 20m class. After the launch, IKAROS performed the deployment sequence and have confirmed that the membrane was successfully expanded. In this paper, the flight data and observed dynamic motion via deployment are reported. These are compared with the results of numerical simulations using multi-particle model, and the accuracy and availability of this model is discussed.

Nomenclature

(x,y,z)	=	coordinate frame fixed to main body
F	=	inter-particle force
β	=	coefficient of dumping
α	=	coefficient of compression stiffness
K	=	spring constant of membrane
L	=	distance between two particles
L_0	=	natural length of spring
M	=	main body's mass
(Ixx, Iyy, Izz)	=	moments of inertia of main body
(Ixy, Iyz, Izx)	=	products of inertia of main body
(x_g, y_g, z_g)	=	center of mass of main body
E	=	Young's modulus of membrane
ν	=	Poisson's ratio of membrane
ρ	=	density of membrane
h	=	thickness of membrane
E_t	=	Young's modulus of tether
d	=	cross section diameter of tether
t	=	time
$(\omega_x, \omega_y, \omega_z)$	=	angular velocity vector of (x,y,z) frame with respect to reference frame
$\boldsymbol{F_d}$	=	damping force of vibration of membrane
θ	=	vibration angle of membrane
κ	=	damping coefficient of vibration of membrane
$\boldsymbol{r_0}$	=	position vector of the root
$\boldsymbol{r_1}$	=	position vector of the first node

I. Introduction

JAPAN Exploration Agency (JAXA) launched a powered solar sail "Interplanetary Kite-craft Accelerated by Radiation Of the Sun (IKAROS)" on May 21, 2010. This spacecraft is on a mission to demonstrate technologies

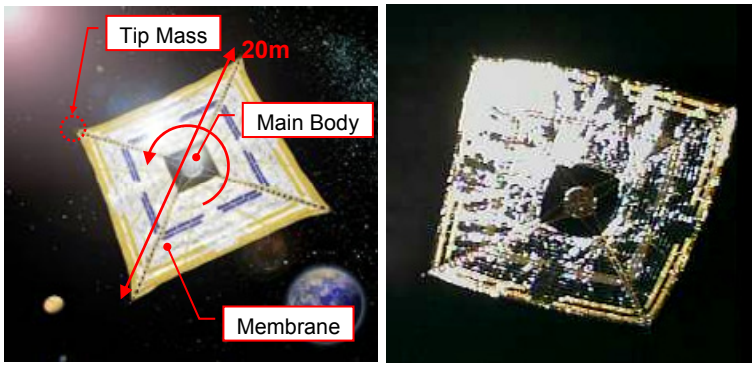

Figure 1. IKAROS, left: illustration, right: image taken by a separation camera.

required at powered solar sail explore mission in the late 2010s. One of the primal technologies demonstrated at IKAROS is the deployment of the sail whose diameter is 20m class. IKAROS performed the deployment sequence and have confirmed that the sail was successfully expanded (Fig.1).

There are some methods to deploy the large membrane, and JAXA is studying the spin type solar sail, in which the membrane is deployed and maintained flat by the centrifugal force. This method is expected to be realized with simpler and lighter-weight mechanism than other ways, because it does not require rigid structural elements. This method also has a risk of instability of main body's attitude or membrane's behavior.

It is very difficult to investigate the dynamics of membrane on the ground because it is greatly affected by air drag and gravity. To solve the problem, some experiment using high altitude balloon or sounding rocket have been conducted[1,2], however the free spin deployment of 20m class of membrane was first experimented by IKAROS.

The shape of the sail developed for IKAROS is a square which consists of four trapezoidal petals. The folding line of each petal is normal to the direction of centrifugal force. Four masses are attached to the four tips of the membrane by tethers to increase the centrifugal force and the inertial momentum of the sail. The sail is connected to the main body by tethers so as not to collide with the main body after the deployment.

Figure 2 shows the deployment method of membrane of IKAROS. The deployment sequence is divided into two major stages. In the first stage, rolling petals are extracted like a Yo-Yo despinner, and form a cross shape

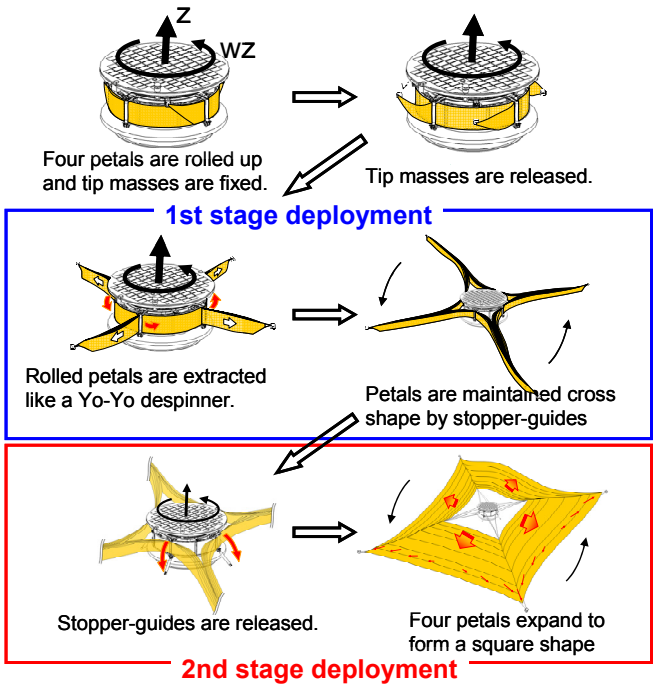

Figure 2. Deployment sequence of IKAROS.

maintained by four rotating stopper guides. In the second stage, these guides are released, and four extended petals form a square shape. If the first stage deployment is performed dynamically, each petal will be twisted around the main body just after the deployment. Therefore the membrane needs to be deployed quasi-statically at the first stage. On the other hand, it is supposed to be deployed dynamically at the second stage. Thus the deployment sequence in IKAROS consists of static first stage and dynamic second stage.

In order to analyze the dynamics of membrane and to organize a detailed deployment sequence, several numerical simulations using multi-particle model were performed before the launch. To find out the effect of the approximation on multi-particle model, numerical simulations using finite element method (FEM) model were also performed. This model was the finite element plane stress model based on the tension field theory, and employed implicit scheme based on the energy-momentum method[3,4]. This model considered the effects of bending stiffness of components on the base membrane and the crease stiffness of folding line. The global behavior of the membrane calculated by FEM model was nearly equal to those calculated by multi-particle model[5], however the validity of simulation using this model had not been established because experiments using large flexible membrane in space

environment. In this paper, the flight data of IKAROS is compared with the results of numerical simulation by multi-particle model, and the validity of the model is evaluated.

II. Multi-particle model

A. Mass-Spring model

In multi-particle model, each element of the membrane is assumed to be isotropic and substituted by particles connected by springs and dampers. This approximation facilitates the construction of model and lowers the computational cost. Mass of each particle is determined based on a designed value and actual measured value, and ununiform mass distribution of sail and difference of four petal's mass are considered.

The inter-particle force F can be described as following form:

$$F = \begin{cases} K(L - L_0) + \beta K\dot{L} & (L \geq L_0) \\ K\alpha(L - L_0) + \alpha\beta K\dot{L} & (L < L_0) \end{cases} \tag{1}$$

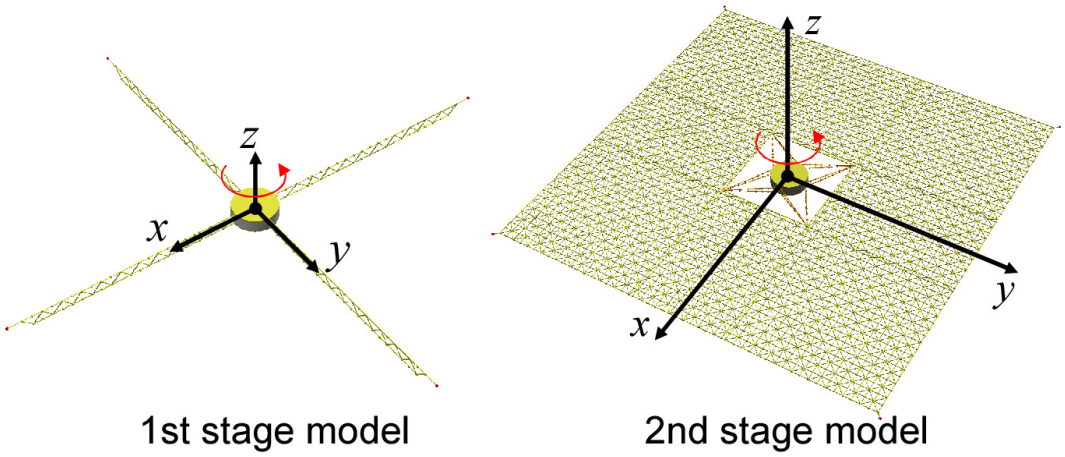

Figure 3. Numerical model for IKAROS.

where K, L, L_0, α and β denote spring constant, natural length of spring, distance between two particles, coefficient of compression stiffness and coefficient of dumping, respectively. Assuming that the membrane resist a compression slightly, nonlinear spring model using coefficients of compression stiffness are employed. The spring constant K are determined by applying the principle of virtual work on an element so as to satisfy the relations of strain energy. This model assumes that the stress in the direction along each spring depends only on the strain in the same direction, so that the elasticity matrix is approximated to be diagonal. This model can also take into account the effect of bending stiffness of each element and crease stiffness of folding line by implementing rotational spring, however these characteristics have little effect on the global behavior of the membrane, and are not considered in this study. For the scheme of numerical time integration, the explicit Runge-Kutta-Gill method is employed.

B. Numerical model for IKAROS

Figure 3 illustrates the numerical models for IKAROS. This models consists of rigid main body and membrane and tethers are mass-spring model. The coordinate frame *(x, y, z)* is fixed to the main body and it's origin is set to the geometric center of the main body. Parameters of the model are shown in Table 1. The coefficients of damping and compression stiffness are unknown parameters. The alignment of mass point and spring are differ between first stage deployment model and second stage deployment model. The positions of mass points and the connections of springs of a quarter part of membrane and tethers for each model are shown in Figs. 4 and 5, respetively.

Table 1: Parameters of model

Parameter name	Symbol	Value	Unit
mass of main body	M	302.11	kg
iniertia moment of main body	(Ixx, Iyy, Izz)	(47.91, 47.46, 66.44)	kgm^2
product moment of main body	(Ixy, Iyz, Izx)	$(-6.3x10^{-4}, 4.6x10^{-5}, 1.6x10^{-3})$	kgm^2
center of mass	(x_g, y_g, z_g)	$(-1.6x10^{-4}, 2.6x10^{-4}, -2.7x10^{-2})$	m
mass of membrane	M_m	14.253	kg
Young's modulus of membrane	E	3.0	GPa
Poisson's ratio of membrane	ν	0.4	-
density of membrane	ρ	1420.0	kg/m^3
thickness of membrane	h	7.5	um
Young's modulus of tether	E_t	100.0	GPa
cross section diameter of tether	d	0.73	mm

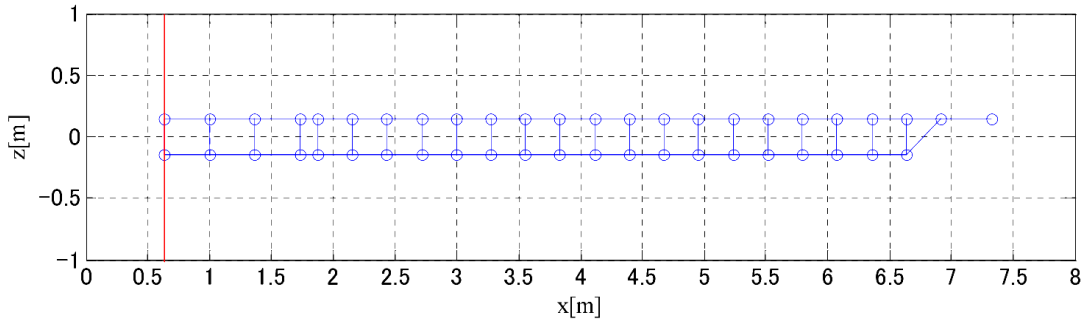

Figure 4. Alignment of mass points and springs of first stage deployment model.

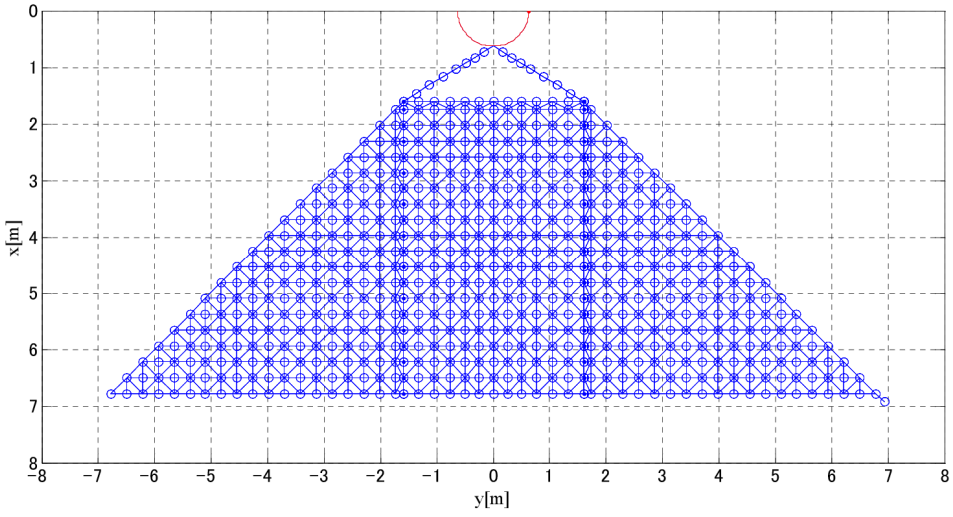

Figure 5. Alignment of mass points and springs of second stage deployment model.

III. Result of deployment operation of IKAROS

This section describes the flight data and observed dynamic motion via deployment operation. After the launch of IKAROS on May 21, 2010, the membrane deployment operation was conducted as follows:

May 26 Tip mass separation
May 27~31 Spin up
June 2 First stage deployment #1~2
June 3 First stage deployment #3~6
June 4 First stage deployment #7~9
June 8 First stage deployment #10~11
June 9 Second stage deployment

This operation was conducted checking the data of triaxial rate gyro and the images of monitor camera. Measurement resolution and sampling frequency of the rate gyro is 0.01deg/s and 4Hz, respectively. Monitor camera are consists of four camera-heads (CAM-H1,2,3,4), which can shoot simultaneously and get 360-degree view around the main body. Figure 6 shows the alignment of camera heads.

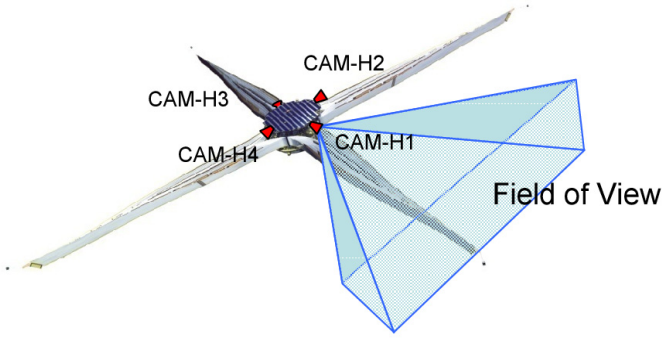

Figure 6. Alignment of camera-heads.

A. First stage deployment

Table 2 shows the operation result of the motor for relative rotation of guides within the first stage deployment. The operation was divided into 11 major steps.

Table 2: Operation of the motor for relative rotation of guides.

Step No.	rotation angle[deg]	Total drive time[s]
#1	10.1	48
#2	21.3	100
#3-1	36.5	170
#3-2	51.7	240
#3-3	66.9	310
#4	112.5	500
#5	158.1	690
#6-1	203.7	880
#6-2	243.4	1040
#7-1	294.9	1252
#7-2	340.5	1444
#8	386.1	1646
#9-1	431.8	1848
#9-2	471.0	2014
#10	530.1	2136
#11	570.0	2222

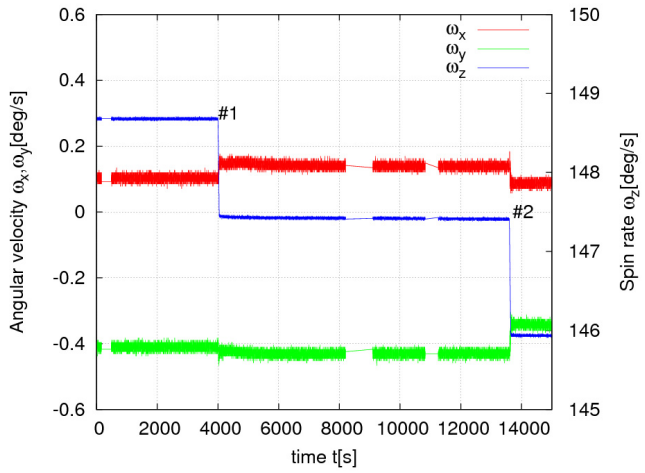

Figure 7. Spin rate and angular velocity of main body during step #1-#2.

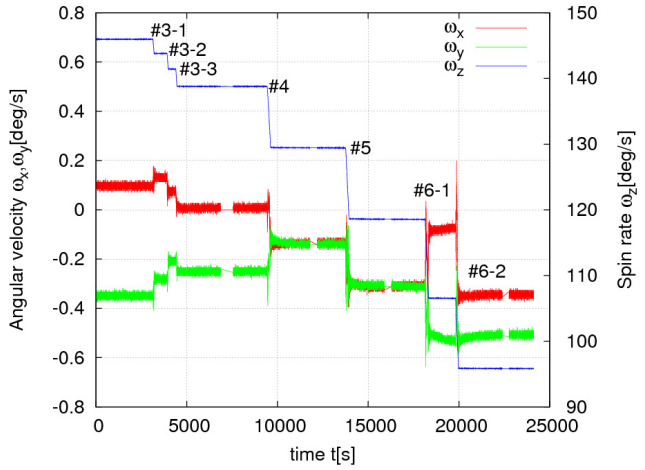

Figure 8. Spin rate and angular velocity of main body during step #3-#6.

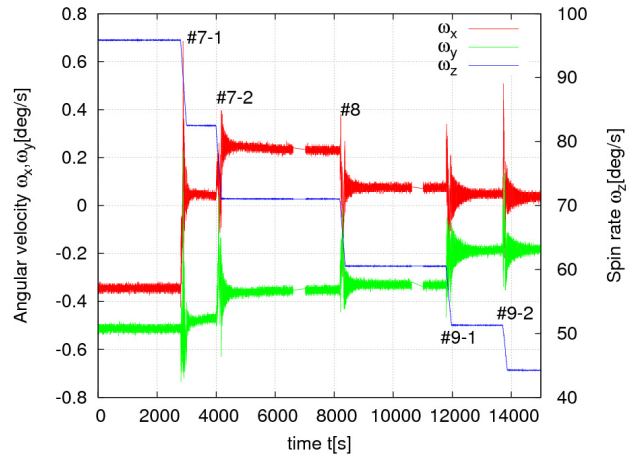

Figure 9. Spin rate and angular velocity of main body during step #7-#9.

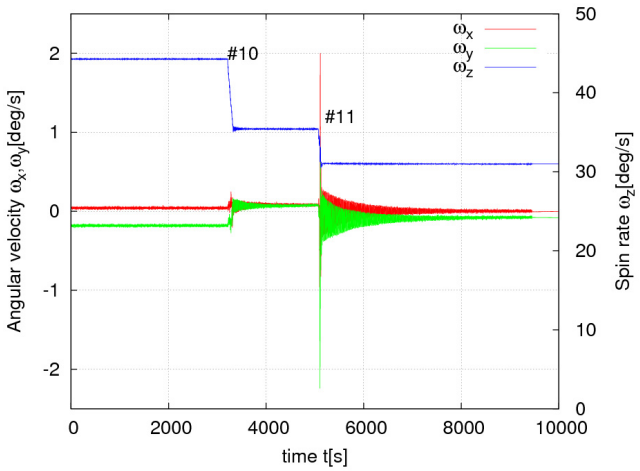

Figure 10. Spin rate and angular velocity of main body during step #10-#11.

Figures 7-10 shows the the flight data of rate gyro within the first stage deployment. The value of ω_x and ω_y oscillate within ± 0.4deg/s for each step with exception of step #11. The spin rate ω_z decrease as the sequence proceed, and it's oscillation is damped quickly. Figure 10 shows the images taken by monitor camera after step #8. These data confirm that the membrane was deployed properly.

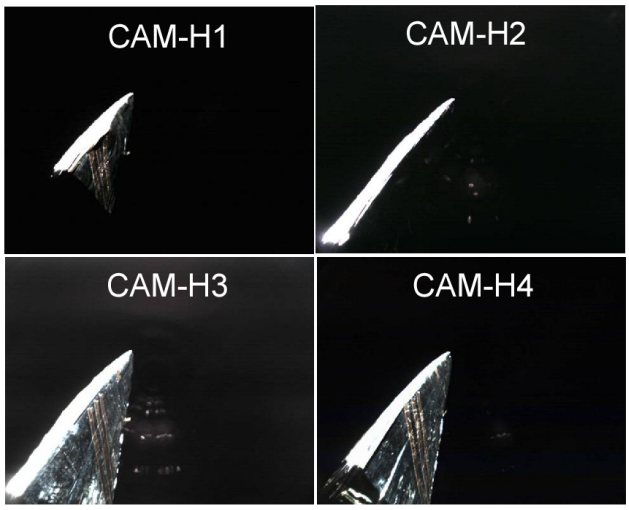

Figure 11. Images by monitor camera taken after step #8.

B. Second stage deployment

Figures 12 and 13 show the flight data of rate gyro within the second stage deployment. The deployment start time is t = 5908.449s in this figure. The value of ω_x and ω_y oscillate irregularly within ± 1.5deg/s while 250s after the deployment start, and then converges to stable nutation with the amplitude of about ± 0.5deg/s and the frequency of about 13.5 deg/s. This nutation motion is dumped gradually, and it takes more than 16000s to converge.

The center of oscillation of ω_z seems to change from 18deg/s to 15deg/s at about 25s after the deployment start. Figure 13 shows the continuous shot images of membrane taken by monitor camera during the second deployment. By checking these images, it turned out qualitatively that the deployment was proceeded asymmetric and membrane between CAM-H1 and 2, and between CAM-H2 and 3 were not expanded until the time. From these data, it is

reasonable to consider that the second stage deployment was proceeded asymmetric and two of petals were not expanded until about 25s after the release of guides. The cause of this deployment stuck is under the investigation. Though the membrane was deployed asymmetric and discontinuously, the sail was expanded completely.

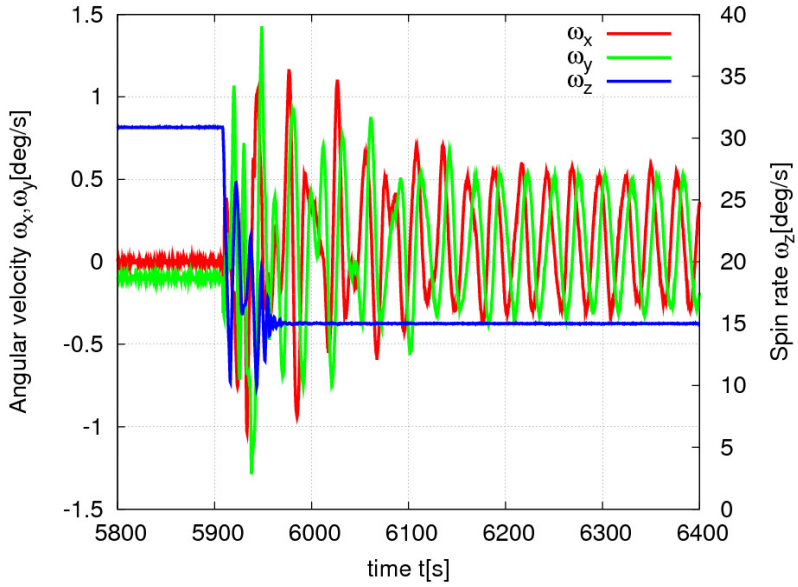

Figure 12. Spin rate and angular velocity of main body during the second stage deployment.

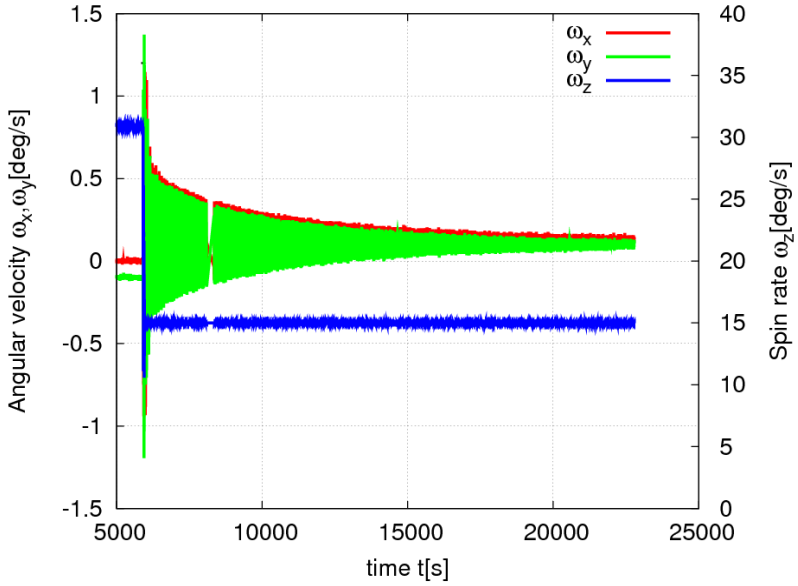

Figure 13. Dumping of angular velocity of main body after the second stage deployment.

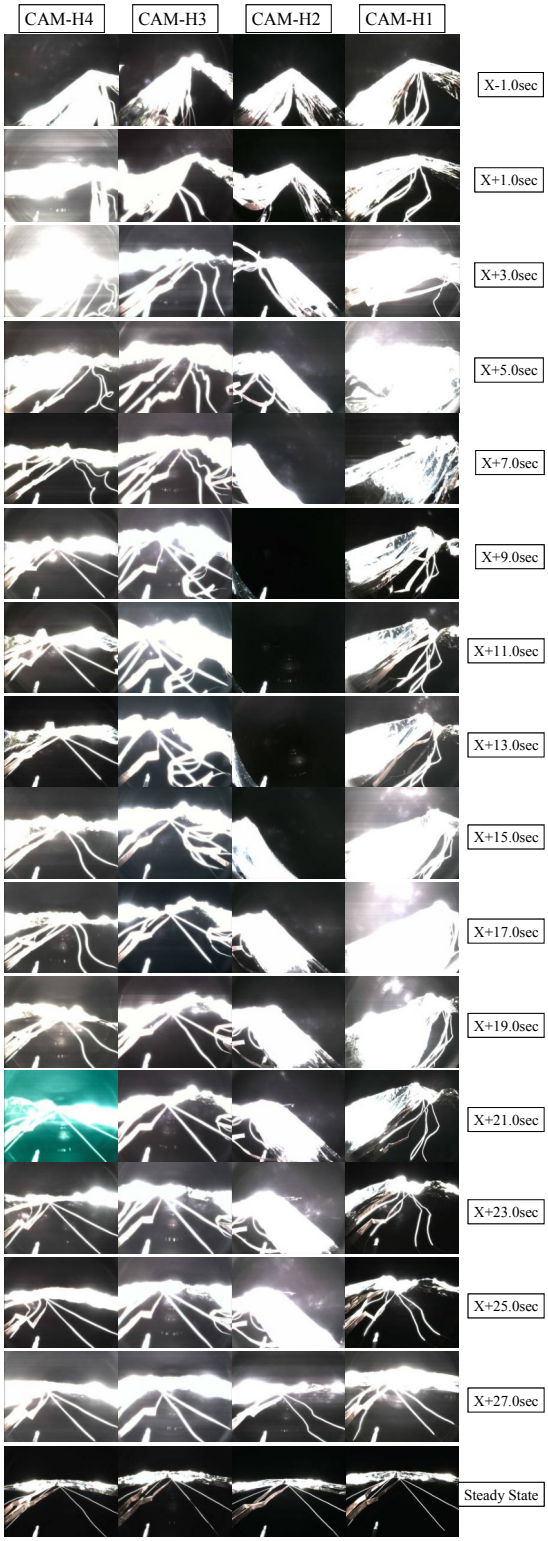

Figure 14. Continuous shots by monitor camera in the second stage deployment.

IV. Comparison of the result of muti-particle model with the flight data

In this section, the results of simulation using multi-particle model are compared to the flight data.

A. First stage deployment

Figure 15 shows the variation of spin rate with respect to the rotation angle of the motor. The decrease of spin rate of simulation result is smaller than the flight data. It would appear that there is an error of estimation of mass

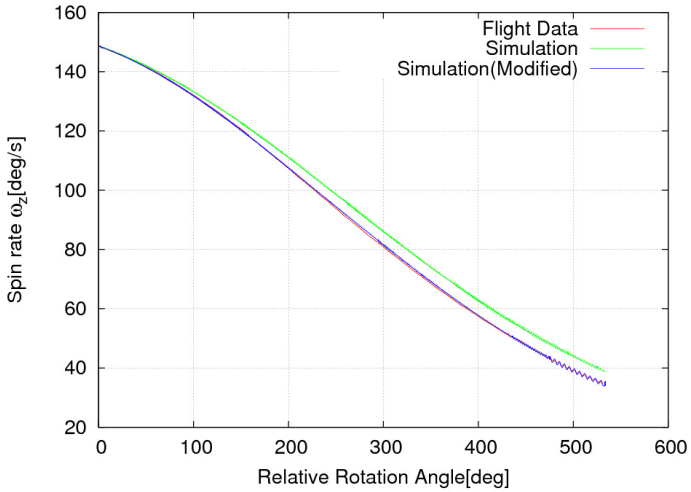

Figure 15. Decrease of the spin rate with respect to the rotation angle of the motor.

distribution for simulation model. To adjust the simulation result to the flight data, the authors derive a modified mass distribution model after several trial-and-error iterations, as shown in Fig. 16. The error of spin rate after each step between the result of modified simulation model and the flight data is reduced to less than 0.5deg/s as shown in Fig. 15.

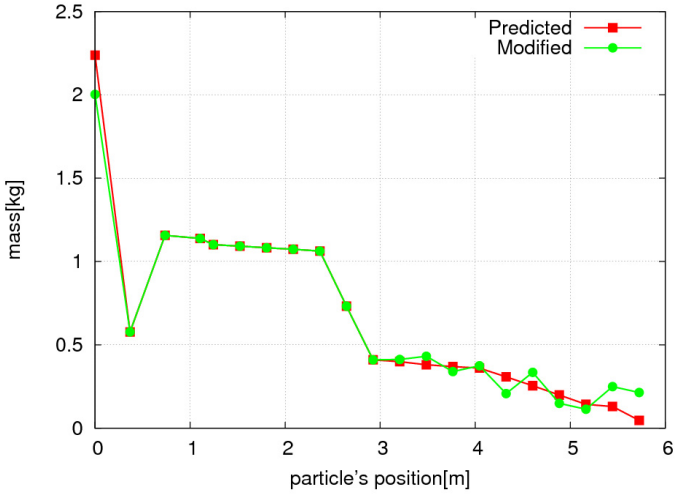

Figure 16. Mass distribution of the first stage deployment model.

Figure 17 shows the oscillation of spin rate after step #10. The spin rate of flight data is oscillated after each step

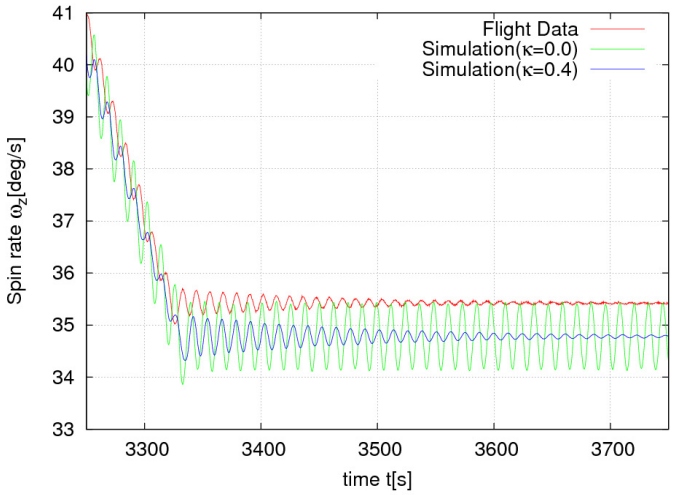

Figure 17. Comparison of the damping of spin rate after step #10.

and then damped quickly. The damping ratio of the spin rate after step #10 obtained by curve-fitting is about 0.0127. This quick damping can not be simulated by the multi-particle model though the coefficient of damping of membrane is varied over a wide range. To simulate this quick damping, the authors apply a damping force model which is proportional to the change rate of vibration angle of membrane. The concept of the model is illustrated in Fig. 18. The damping force F_d of this model can be expressed as follows:

$$\mathbf{F}_d = -\kappa\dot{\theta}\frac{(\mathbf{r}_1-\mathbf{r}_0)\times\{(\mathbf{r}_1-\mathbf{r}_0)\times\dot{\mathbf{r}}_1\}}{\left\|(\mathbf{r}_1-\mathbf{r}_0)\times\{(\mathbf{r}_1-\mathbf{r}_0)\times\dot{\mathbf{r}}_1\}\right\|} \tag{2}$$

where κ, $\mathbf{r_0}$ and $\mathbf{r_1}$ denote the damping coefficient of vibration of membrane, the position vector of the root and the first node, respectively. θ is the vibration angle of membrane defined as the angle between $\mathbf{r_0}$ and $(\mathbf{r_1}\text{-}\mathbf{r_0})$. The result of simulation which employs this model with κ=0.4 is also shown in Fig. 17. The damping ratio of the spin rate is obtained as 0.013, which is nearly equal to the one of flight data.

Thus the modified multi-particle model can simulate the global behabiour of main body during the first stage deployment well.

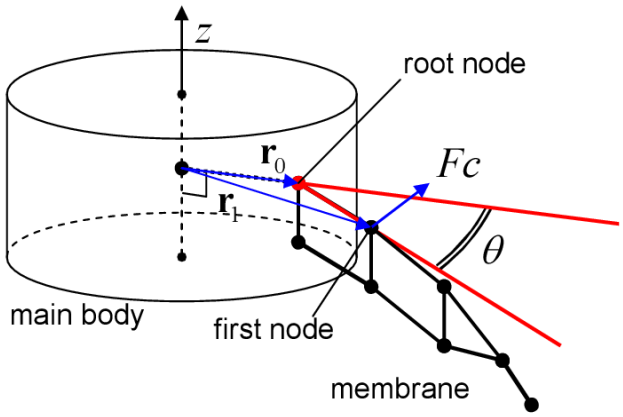

Figure 18. Model of damping force proportional to the change rate of vibration angle of membrane.

B. Second stage deployment

As described in previous section, it is reasonable to consider that the second stage deployment was proceeded asymmetric and two of petals were not expanded until about 25s after the release of guides. To simulate the this feature of flight data of rate gyro, a simulation which appended a force of constraint that two petals not to expand for 26s after the deployment sequence start was performed. Figures 19 and 20 show the result of the simulation compared to the flight data. The amplitude of ω_x and ω_y of simulation is the same level of the flight data. The shift of center of oscillation of ω_z of flight data is also well simulated by the model includes the constraint.

The flight data shows the value of ω_z is converged quickly about 60s after the deployment start. This quick dumping of the oscillation of ω_z is not well simulated as shown in Fig. 20. A dumping coefficient β of membrane in this simulation is 2.0×10^{-4}s. Though it was much higher than that of normal case specified before the launch, the oscillation of ω_z was not dumping so quickly as the flight data. If the membrane's motion is affected by the strong dumping force, the membrane converges to the expanded shape quickly and then an in-plane oscillation between the main body and the membrane is induced. In such case, high tension is applied to the membrane and then the

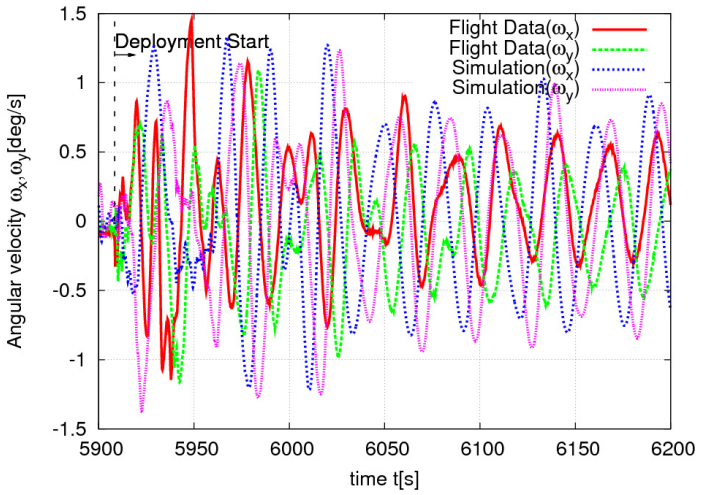

Figure 19. Comparison of the angular velocity of simulation result and flight data.

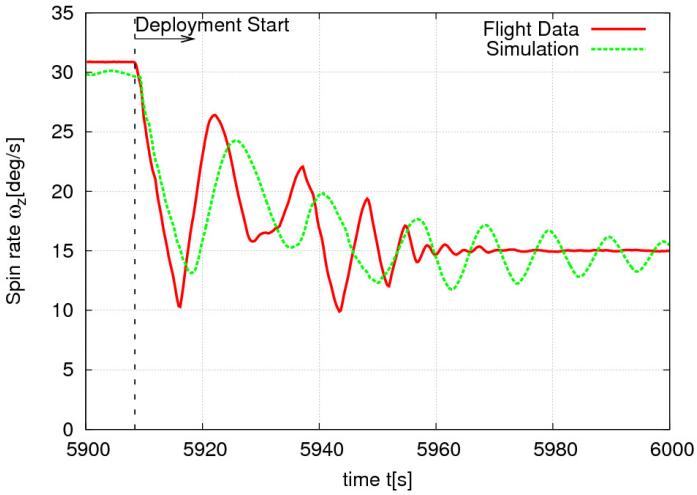

Figure 20. Comparison of the spin rate of simulation result and flight data.

accuracy of prediction of motion by multi-particle model would become worse because it uses diagonal approximated elasticity matrix. To simulate the dumping behavior with multi- particle model, some improvement would be needed.

V. Conclusion

JAXA launched a powered solar sail "IKAROS" on May 21, 2010 and succeed the deployment of membrane. In this paper, flight results of the deployment was reported and compared with the results of numerical simulations using multi-particle model. It was found that multi-particle model could simulate the global behabiour of membrane well, except the dumping of in-plane oscillation between the main body and the expanded membrane. To simulate this motion well, some improvement would be needed. Outside of this exception, it can be said that the numerical analysis using multi-particle model is feasible to investigate the macro-dynamics of membrane.

References

[1]Y. Tsuda, O. Mori, S. Takeuchi and J. Kawaguchi, "Flight Result and Analysis of Solar Sail Deployment Experiment using S-310 Sounding Rocket," Space Technol., Vol.26, Nos.1-2, pp. 33-39, 2006.

[2]S. Nishimaki, O. Mori, M. Shida and J. Kawaguchi, “Stability and Control Response of Spinning Solar Sail-craft containing A Huge Membrane,” 57th International Astronautical Congress, IAC-06-C1.1.07, Valencia, Oct. 2-6, 2006.

[3]Simo, J. C. and Tarnow, N., "The discrete energy-momentum method. Con-serving algorithms for nonlinear elasto-dynamics," Journal of Applied Mathematics and Physics (ZAMP), Vol. 43, pp.757-792, 1992.

[4]Miyazaki, Y. and Kodama, T., "Formulation and Interpretation of the Equation of Motion on the Basis of the Energy-Momentum Method," Journal of Multi-body Dynamics, Vol.218, pp.1-7, 2004.

[5]Miyazaki, Y. and Iwai, Y., “Dynamics Modeling of Solar Sail Membrane,” 13th Workshop on JAXA Astrodynamics and Flight Mechanics, No. A-6, Kanagawa, Japan, July 2004.